OPPORTUNITIES FOR MICROSTRUCTURAL DEVELOPMENT IN Si_3N_4 CERAMICS

G. Petzow and M.J. Hoffmann

Max-Planck-Institute for Metals Research
Institute for Material Science
Powder Metallurgical Laboratory
Heisenbergstr. 5, W-7000 Stuttgart 80, Germany

The microstructural optimization of high strength, high temperature Si_3N_4 ceramics are discussed. It is demonstrated that microstructural development is predominantly controlled by the properties of the Si_3N_4 starting powder and the sintering temperature, whereas the sintering additive composition has only a minor influence.

Optimum conditions for the growth of Si_3N_4 grains with a needle-like morphology is analysed in sintered specimens as well as in oxynitride glasses. The growth kinetics during α/β transformation and Ostwald ripening have been determined on isolated Si_3N_4 crystals embedded in supersaturated Y-Si-Al-O-N glasses. Finally a crystallization model is introduced to describe the growth mechanisms in relation to the Si_3N_4 crystal structure. It is demonstrated that a fine-grained Si_3N_4 has the highest potential for high strength properties.

Degradation of the Si_3N_4 properties at temperatures > 1200°C is mainly influenced by the chemistry of the grain boundary phase. Therefore the importance of a more complete understanding of phase relationships in the Si_3N_4-sintering additive ceramic systems is necessary. TEM observations reveal an amorphous grain boundary film in two-grain junctions even in "fully" crystalline Si_3N_4 ceramics. The equilibrium thickness of these amorphous layers depends on the chemistry of the sintering additives and is expected to control the high temperature properties.

INTRODUCTION

Silicon nitride-based ceramics exhibit excellent mechanical properties, good oxidation resistance and thermal shock behaviour at room and high temperatures. The high wear resistance and the mechanical properties of these ceramics are interesting for several applications.

The properties of silicon nitride ceramics depend upon its bulk density. The highly covalent bonding of Si_3N_4 results in a low self-diffusion coefficient of the nitrogen atoms of $6.3 \cdot 10^{-20}$ cm^2/s at 1400°C [1], hence it follows that a densification without any sintering additives is nearly impossible. In 1961, Deeley, et al. [2] was the first to report that Si_3N_4 ceramics could be densified by hot-pressing with the addition of oxides as sintering additives. Today, it is common practice to densify Si_3N_4 by pressureless sintering, gas pressure sintering, hot-pressing or hot isostatic pressing. The sintering aids are usually metal oxides such as MgO, Al_2O_3 and most of the rare earth oxides [3-7].

The densification is described as a liquid phase sintering process. At higher temperatures, SiO_2, which is always present at the surface of the Si_3N_4 particles [8], reacts with the oxide additives to form an oxide melt and, with increasing temperature, an oxynitride melt by dissolving Si_3N_4. After the α-Si_3N_4 particles dissolve and supersaturate the liquid phase, β-Si_3N_4 is reprecipated [9]. Depending upon the composition of the sintering aids, the liquid phase can form an amorphous or a crystalline grain boundary phase during cooling both of which degrade the mechanical properties of the Si_3N_4 at temperatures > 1000°C, because of the drastic softening of the grain boundary regions [10,11].

Oyama, et al. [12,13] and Jack, et al. [14] tried to overcome the problem of high temperature strength degradation by investigating the solid solution between Si_3N_4 and Al_2O_3. The idea was the preparation of a single phase so-called "SiAlON" ceramic without an amorphous grain boundary. The crystal structure of β-SiAlONs can be derived from the β-Si_3N_4 lattice by a simultaneous replacement of Si^{4+} by Al^{3+} and N^{3-} by O^{2-}. Furthermore, Huseby, et al. [15] reported the existence of an extended solid solution between Si_3N_4 and BeO. Other sintering additives such as MgO or Y_2O_3 show no appreciable solubility in the β-Si_3N_4 lattice.

In comparsion to the β-SiAlONs, there is a remarkable solubility of rare earth ions in α-SiAlONs due to the different crystal lattice structure of α-Si_3N_4 [16]. The α-SiAlONs offer the possibility of incorporating the sintering additives and impurities into the structure resulting in a sintered, single-phase ceramic [17]. α-SiAlONs exhibit better thermal shock resistance [18] and

higher hardness [19] in comparsion to ß-Si_3N_4 based ceramics. These properties offer a great potential for application as cutting tools.

The characteristic microstructure of Si_3N_4, containing elongated grains with high aspect ratios, is responsible for the excellent mechanical properties, especially at room temperature. The development of this type of microstructure can be explained by the crystal structure of ß-Si_3N_4 and its growth mechanisms. It is possible to achieve an "in-situ whisker reinforcement" by the control of anisotropic grain growth, so that Si_3N_4 ceramics exhibit high fracture toughness [20]. The alternative way to reinforce Si_3N_4 with SiC whiskers is not a promising route because of the difficulties of obtaining a homogeneous whisker dispersion and the problems of densification [21,22].

The purpose of the present paper is to discuss the relationship of two important factors, microstructure development and phase relationships, in Si_3N_4-based ceramics and their influence on the mechanical properties.

MICROSTRUCTURAL DEVELOPMENT

The influence of the microstructure of β-Si_3N_4 on the mechanical properties has been well-known since the 1970's and results show that a needle-like grain morphology is desirable [23]. Faber and Evans [24,25] calculated the influence of the aspect ratio on the fracture toughness. This theory could be applied in principle to the microstructure of Si_3N_4. If the fracture mode is intergranular, a deflection of the direction of the propagating crack increases the fracture surface energy. Therefore, the fracture toughness increases with an increasing aspect ratio of the Si_3N_4 grains.

Influence of the α/β ratio in the initial powder

Detailed studies on grain growth phenomena have been performed only in the last 5 years. F.F. Lange [23] investigated hot-pressed Si_3N_4 with 5 wt.% MgO and found that the aspect ratio of the grains and, therefore, the fracture toughness was determined by α/β ratio in the starting Si_3N_4 powder. The

ıce of the α/β ratio is also detectable in the microstructure of ·eless sintered samples. The SEM micrograph in Fig.1 reveals a needle-.crostructure on the left-hand side and a fine-grained microstructure on ght-hand side.

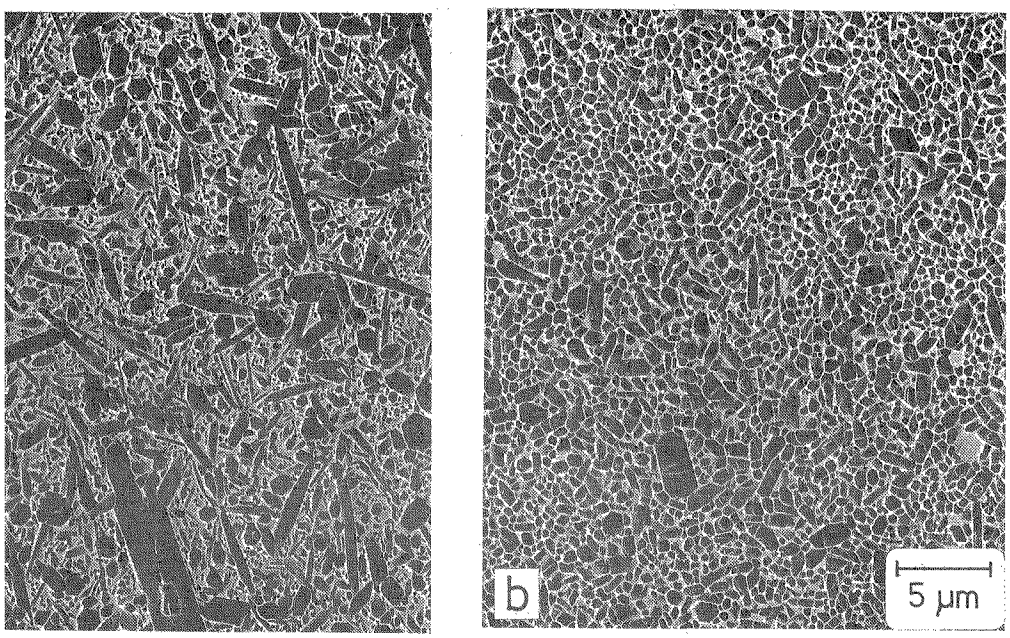

1: SEM-micrograph of pressureless sintered Si_3N_4 with a starting powder of 95% α- / 5% β-phase (a) and 100% β-phase (b).

geneous nucleation of ß-crystals during densification does not play a cant role. This can been seen if we calculate the number of β-nuclei (D_F) in the starting powder by the simple relationship [26]

$$D_F = \frac{3}{2} \frac{\beta \cdot \rho_s}{\pi \cdot (r_N)^2 \cdot \rho_{SN} \cdot 100} \qquad (1)$$

ıer the assumption that the β-particles have the same mean particles ı the starting powder as the α-particles. β denotes in equ. (1) the content in the initial powder, ρ_s the theoretical density of the :d specimen, and ρ_{SN} the density of Si_3N_4. (r_N) is mean particle size of

the Si_3N_4 powder. Table 1 shows a comparison of the calculated β-nuclei de sity (N) for different commercial Si_3N_4 powders in comparison to the measur particle density after sintering.

Si_3N_4 powder	Nucleation Density	Particle Density
UBE E 10	5.50	4.90
UBE ESP	<1.65	1.37
Starck LC 12-S	3.84	2.51

Table 1: β-nuclei density and β-particle density for different commercial Si_3N_4 powders [26]

Table 1 shows a relative good agreement between the calculated β-nucl density and the measured β-particle density. Differences could be explained the solution of smaller grains during Ostwald-Ripening in the last stage sintering.

The assumption that only β-crystals grow was checked by experimental studi of pressureless sintered samples with fine- grained starting powder (me grain size 0.5 μm), which was doped with 5 vol.% of α-Si_3N_4 with a mean gra size of 1 μm. Specimens with 10 wt.% sintering additives (Y_2O_3/Al_2O_3) we densified at 1700°C and 1800°C. The SEM analysis showed that the coar α-particles dissolve only in the later stage of sintering due to the stability in comparison to smaller α-particles. There were no coarse particl detectable which could act as a heterogenous nuclei for a needle-like growi β-grain. Figure 2 shows an SEM micrograph of the specimen. The α-particl show particle disintegration and coexist in the near fully-densified a partially transformed microstructure, with the typical elongated β-grai which were formed by dissolution of the smaller α-particles and reprecip tation at preexisting β-crystal planes.

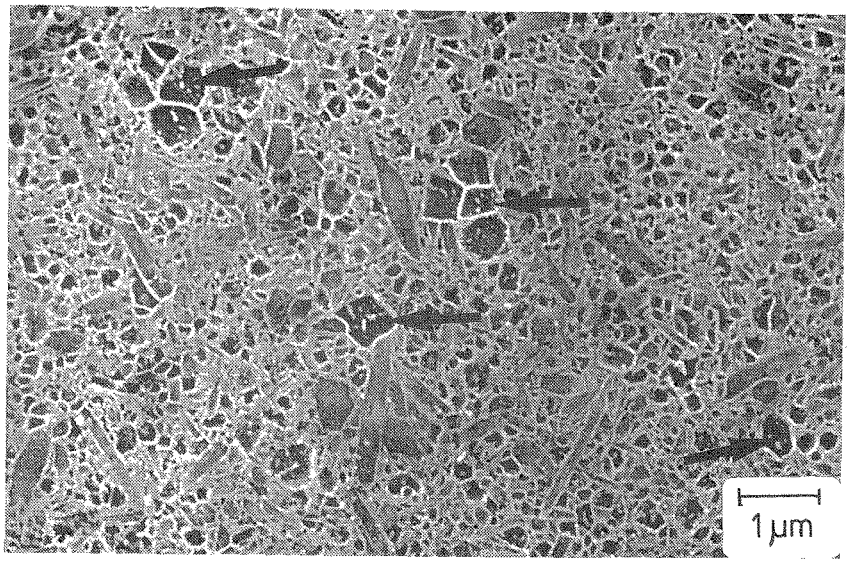

Figure 2: Plasma-etched Si_3N_4 specimen with coarse unreacted α-particles (marked by arrows) after 1h isothermal sintering at 1800°C.

Growth Mechanisms

Krämer, et al. [27] made an detailed analysis of the grain growth mechanisms related to the anisotropy of the β-Si_3N_4 crystal structure. Describing the growth mechanisms during sintering on the basis of the crystallisation model of Kossel and Stranski [28], a remarkable discontinuous grain growth of β-Si_3N_4 was found as well as different growth rates of the basal plane (perpendicular to the c-axis of β-Si_3N_4) and the prism plane (parallel to the c-axis), which causes the typical elongated grains at temperatures higher than 1800°C. Krämer's observations in plasma-etched samples can be summarized as follows

i) A higher growth rate of the basal plane in comparsion to the prism plane in the area of a liquid phase.

ii) The grain growth of the basal plane stops when it hits a prism plane (Fig. 3a and 3b marked with arrows).

iii) The prism planes are dominant and they grow by dissolution of the basal plane.

iv) If the basal plane of a large crystal surrounds the prism planes of a smaller one, the small grain will dissolve.

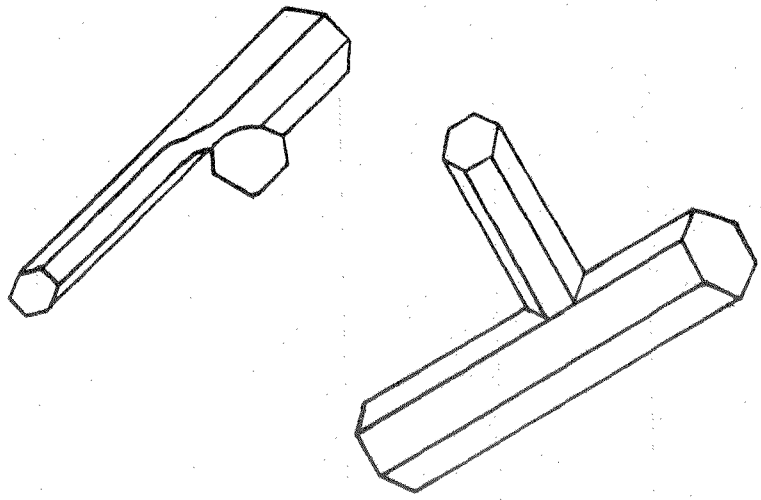

Figure 3a: Schematics of different oberservations.

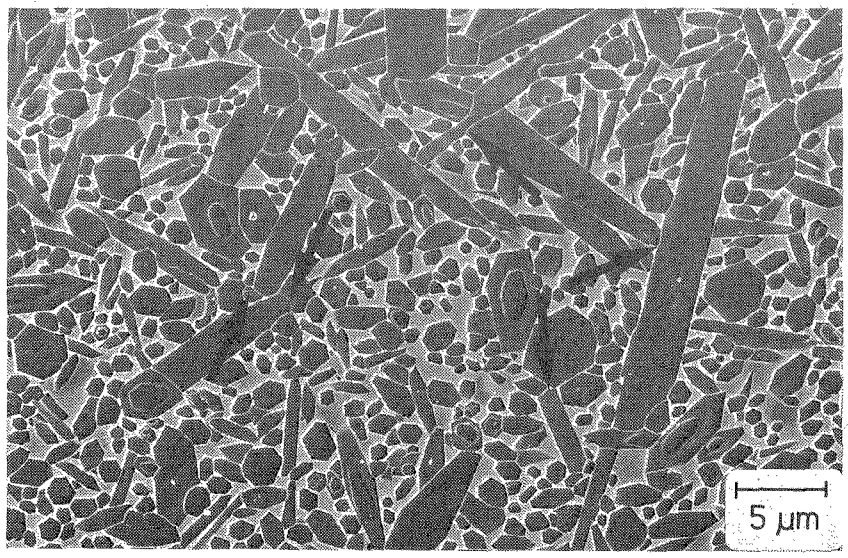

Figure 3b: Presureless sintered and plasma-etched Si_3N_4 sample.

Figure 3a and b: Grain growth mechanisms in Si_3N_4 ceramics.

The growth phenomena were explained by consideration of the β-crystal structure. Characteristic is the high covalent bonding of 70%, a c/a ratio of the lattice constants < 1 and the different stacking of the nitrogen atoms in the a- and c-direction (a: ABCABC... and c: ABAB...). The packing density

thin the layers perpendicular to the c-direction and the distance of the yers is relatively low [29]. The opposite is valid for the layers perpendilar to the a-axis. The different distances of the layers and their packing ısity indicates an anisotropy of the boundary energy and different stabi-:ies of the prism and basal plane. Under Krämer's consideration of the ssel & Stranski model, the crystal grows by attachment of discreet growth its which have the tendency to minimize their energy. The anisotropy in ındary energy estimated from the number of bonds per unit area parallel and pendicular to the c-axis is represented in Fig. 4 by small rectangles. For :h crystal planes, the rate-determining step is the surface nucleation.

demonstrated in Fig. 4, the energetically more favourable surface :leation on the basal plane results in higher growth rates there in compason to the prism plane. A growth of the layer within the prism plane is very st if nucleation occurs.

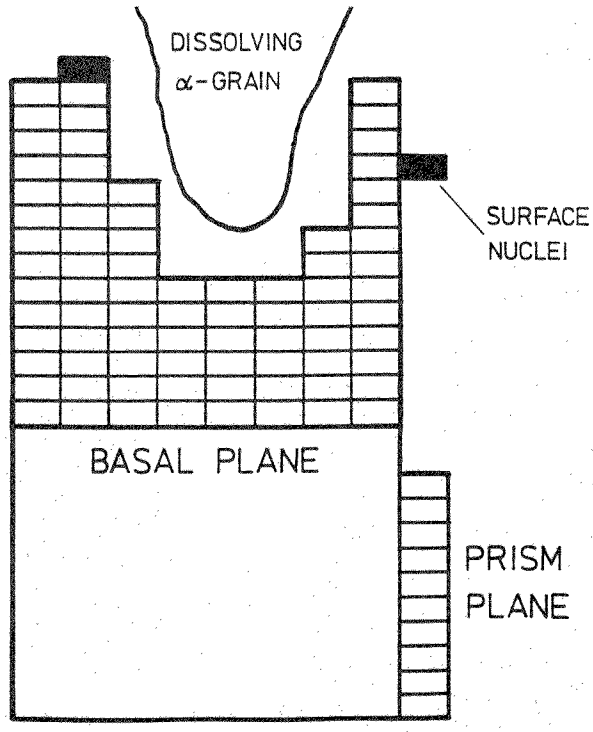

gure 4: Schematic of the kinetic growth model for elongated β-Si_3N_4 grains. The small rectangles represented the anisotropy of energy between the layers parallel and perpendicular to the c-axis.

The model predicts that the prism plane is more stable than the basal plane. This explains why the prism plane is dominant and stops the discontinuous grain growth of basal planes. Furthermore, it is possible to assume that the aspect ratio of the β-grains increases when the grains grow (in thermodynamic nonequilibrium). For longer isothermal sintering times the microstructures reach thermodynamic equilibrium and the aspect ratio decreases. This effect was experimentally found by Wötting et al. [30].

Grain Growth Studies in Oxynitride Glasses

A disadvantange of the grain growth investigations in sintered microstructures is the steric hindrance of the growth of β-needles by the surrounding grains. Krämer, et al. studied therefore the grain growth behaviour in a very dilute system, such as Si_3N_4-supersaturated oxynitride glasses [31]. These glasses were prepared by a heat treatment of homogenous mixtures of Y_2O_3, Al_2O_3, SiO_2 and Si_3N_4 at 1650°C for 0.5 h. After cooling to room temperature Y-Si-Al-O-N-glasses were subsequently heat treated at 1550, 1600 and 1640°C for 1 to 18 hrs to investigate grain growth. Figure 5 shows an elongated Si_3N_4 grain in an oxynitride glass after a heat treatment of 2 h at 1600°C.

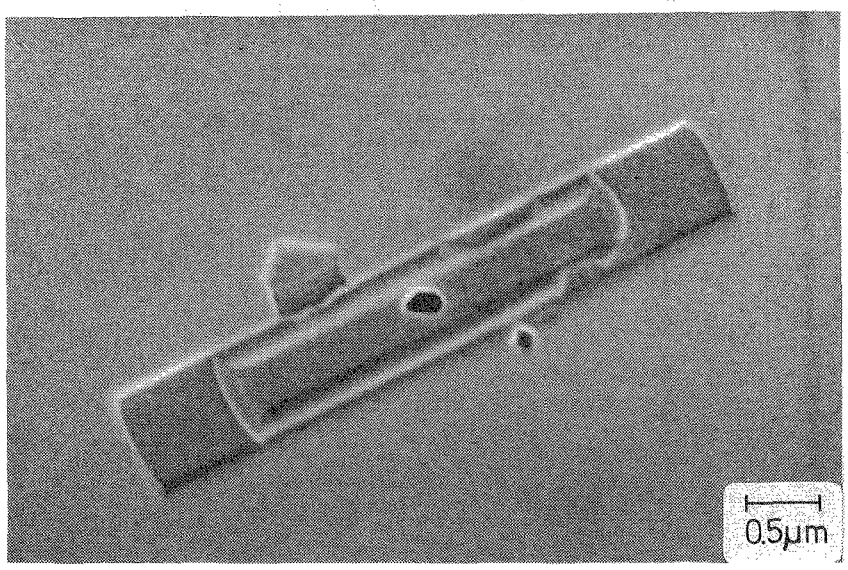

Figure 5: Plasma-etched Si3N4-crystal in a Y-Si-Al-O-N-glass

The grain shows an internal structure with a core in the middle visible after plasma-etching. For the development of the grain structure, three different stages must be considered. The core represents the β-nucleus of the inner crystal growing during the first heat treatment at 1650°C. This crystal has an aspect ratio of about 9. During cooling to room temperature, the bright rim formed equally on the basal plane and the prism plane. A second heat treatment at 1600°C caused a further increase in aspect ratio with a ratio of the growth rate for basal plane to the prism plane of at least 1 to 15.

The quantitative microstructural analysis of the β-Si_3N_4 grains embedded in the Y-Si-Al-O-N glasses revealed that the mean diameter remains constant during isothermal heat treatment. The development of the mean grain length exhibits a strong increase during the α/β-transformation and remains constant or was reduced during the subsequent Ostwald-Ripening depending on the actual temperature [31]. Figure 6 shows the mean aspect ratio of β-Si_3N_4 grains as a function of time for a isothermal heat treatment at 1550°C, 1600°C and 1640°C.

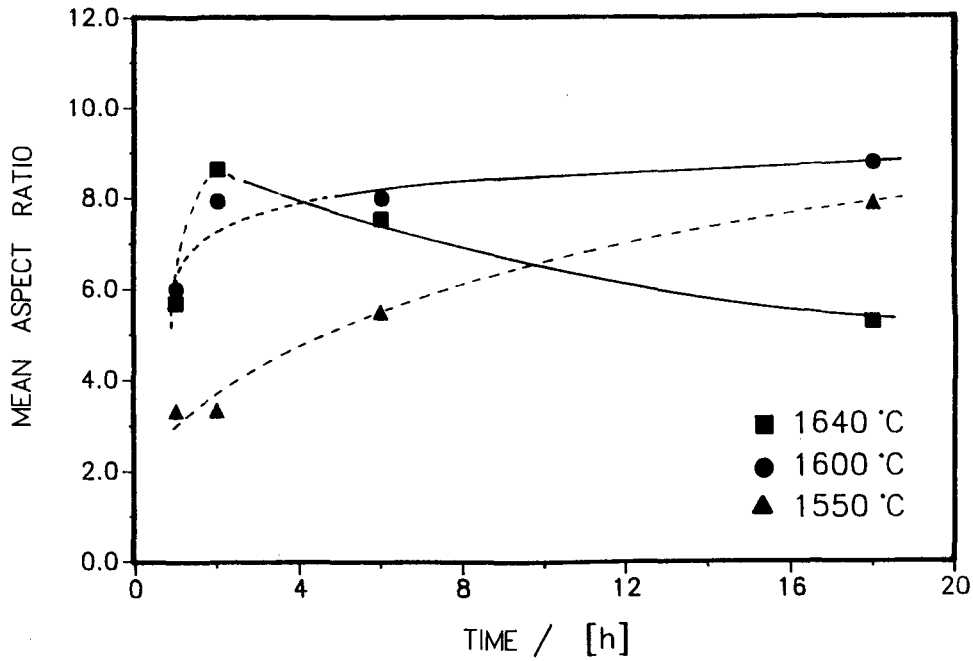

Figure 6: Mean aspect ratio as a function of time for Si_3N_4 grains dispersed in oxynitride glasses.

The dotted lines represent the stage during α/β transformation. After 18 hrs heat treatment at 1550°C, the α/β transformation is still incomplete so that the aspect ratio can increase further. At 1600°C, a strong increase in the aspect ratio is detectable in the late stage of α/β transformation (up to 6 hrs). During the subsequent heat treatment period where Ostwald-Ripening occurs the mean aspect ratio remains nearly constant. The specimens heat treated at 1640°C reveal a decrease in aspect ratio for longer heat treatment times due to the dissolution of grains with small diameters and high aspect ratios.

The quantitative analysis of Krämer, et al. [31] shows that the highest aspect ratios of β-grains dispersed in Y-Si-Al-O-N- glasses could be achieved at the end of the α/β transformation. These experimental results demonstrate clearly that a polycrystalline Si_3N_4-based ceramic should be densified at temperatures as low as possible. Similar to the results in dilute systems it is expected that the grains exhibit the maximum aspect ratio also at the end of the α/β-transformation.

DEVITRIFICATION OF THE AMORPHOUS GRAIN BOUNDARY PHASE

The development of a specific microstructure with a well-defined crystalline grain boundary phase is not possible without the knowledge of the phase relationships of the different phases present after sintering. Unfortunately most of the Si_3N_4-based ceramics are quaternery or quinary sytems due to the necessity of oxide additions as sintering additives. If the valencies of the elements are considered to be fixed and the concentrations are expressed in equivalent percents instead of atomic percents the system can be reduced to a quasiquaternary one which can be represented as a regular prism (Jänecke prism) with the compounds Si_3N_4, SiO_2, AlN, Al_2O_3, MeN and Me_2O_3 (Me = metal) as end members at the six corners [32]. All the interesting phase relationships important for the development of Si_3N_4-based ceramics can be represented in this prism. The interesting isothermal sections are at sintering temperatures between 1700°C and 1950°C and the temperature range from 1150°C to 1350°C for the heat treatments to devitrify the amorphous grain boundary region.

Phase Relationships in Y-Si-Al-O-N Based Ceramics

The reason for the extensive investigations in the system Y-Si-Al-O-N is that yttrium oxide has emerged as one of the best sintering additives for densification of Si_3N_4. A further improvement can be achieved by addition of Al_2O_3 to form β-sialons and highly refractive crystalline grain boundary phases such as YAG [11]. A good summary of previous work in the yttria sialon system has been given by Jack [33] and Thompson [34].

Si_3N_4-based ceramics with Al_2O_3 additives exhibit excellent high temperature properties if the alumina forms a solid solution with the Si_3N_4 (sialon) or is incorporated into a crystalline grain boundary phase. Residual Al_2O_3 in an amorphous grain boundary lowers its viscosity and is responsible for the typical decrease in bending strength of Si_3N_4 in the temperature range between 1000°C and 1200°C as well as the high creep rates. The best high temperature Si_3N_4 with Y_2O_3 and Al_2O_3 as sintering additives contain a high ratio of Y_2O_3 to Al_2O_3 to crystallize the grain boundary phases represented on the oxygen-rich side of the phase diagram Si_3N_4-SiO_2-YN-Y_2O_3 [35] (Fig. 7).

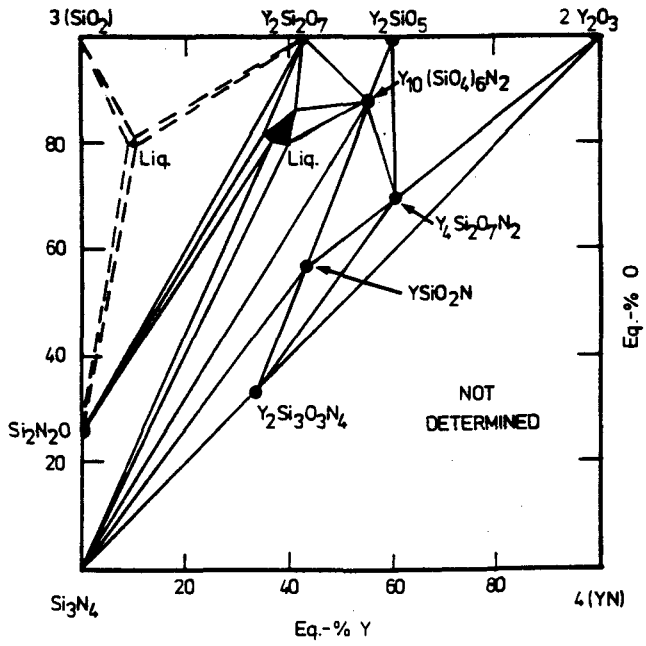

Figure 7: Phase relationships in the Si3N4-SiO2-YN-Y2O3 system at 1550°C after Gaukler et al. [35].

All phases are highly refractory but the compounds within the Si_3N_4-$Y_2Si_2O_7$-Y_2O_3 phase area exhibit relatively large weight gains in air at 1000°C. The catastrophic oxidation behaviour can be explained by a large volume change in these grain boundary phases. The N-melilite ($Si_3N_4 \cdot Y_2O_3$) exhibits the highest volume change ΔV of 33 % [36], calculated according to the oxidation reaction

$$Si_3N_4 \cdot Y_2O_3 + O_2 \longrightarrow Y_2Si_2O_7 + SiO_2 + 2N_2. \qquad (2)$$

For the other nitrogen-containing phases (wollastonite ($YSiO_2N$), J-phase ($Y_4Si_2O_7N_2$) and apatite ($Y_{10}(SiO_4)_6N_2$)), volume changes of 8 %, 10 % and 11 % were determined, respectively. Furthermore, it is assumed that the process which takes place within the oxynitride phase is volume oxidation in contrast to the Si_3N_4 matrix which exhibits surface oxidation. However, the oxidation resistance can be drastically reduced at temperatures > 1300°C and Si_3N_4 ceramics containing oxynitrides as grain boundaries reveal a greater oxidation resistance at 1000°C after a heat treatment at 1350°C [37]. The phenomenon can be explained by the formation of a protective SiO_2 layer at 1350°C from the oxidation of the Si_3N_4 matrix. At 1000°C, Si_3N_4 has a low oxidation rate, thus the SiO_2 layer would be insufficient to cover the oxynitride phase. Quackenbush and Smith [38] showed that the catastrophic oxidation can be avoided by adding a small amount of Al_2O_3 (< 1 wt%). Patel, et al. [36] explained this effect by the low volume change due to the Al-containing oxidation products.

The lowest weight gain was measured on samples with compositions in the triangle $Y_2Si_2O_7$-Si_2N_2O-Si_3N_4. These materials have a grain boundary phase which can not be oxidized. The increase in oxygen content, however, results in poorer high-temperature properties. A compromise is certainly the crystallisation of oxynitride grain boundary phases with a high O/N ratio and a low volume change during oxidation. This can be achieved be adding a small amount of alumina or by changing the sintering additive. For example, the yttrium N-apatite oxidizes with a volume changes of 11.4 % whereas the neodymium N-apatite exhibits a volume change of only 3.3 % [36].

Phase Relationships in Yb-Si-Al-O-N Based Ceramics

Generally, other rare earth oxide-sialon systems have similar phase diagrams to the Y-Si-Al-O-N system. But in some cases there are differences due to the stability of the quasiquaternary phases. Figure 8 shows an isothermal section of the quasiquaternary system Yb_2O_3-SiO_2-Si_3N_4-YbN at 1500°C [39]. There is only one quasiquaternary compound ($Yb_4Si_2O_7N_2$) in comparsion to the 4 phases of the yttrium-related diagram (Fig. 7). The Yb-system has become quite interesting due to the high oxidation resistance of the ytterbia-fluxed materials. Furthermore, the densification of ytterbia-doped Si_3N_4 is easier in comparsion to Si_3N_4 ceramics based on yttria as a sintering additive.

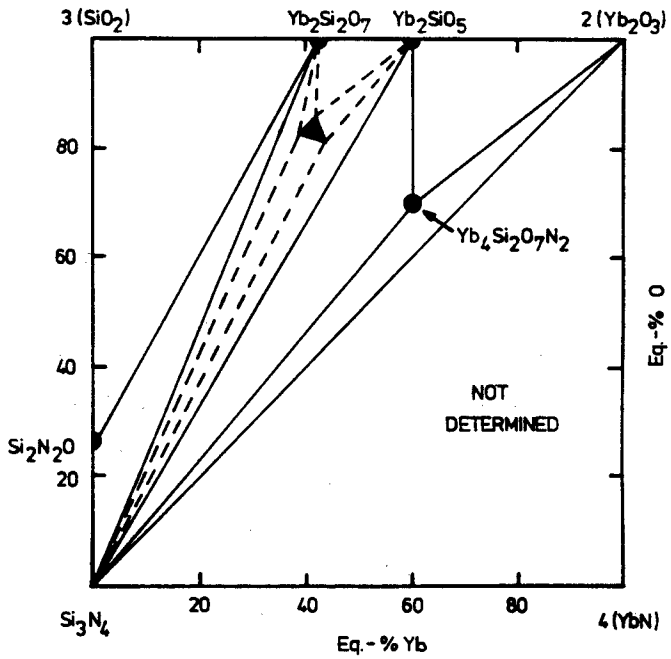

Figure 8: Phase relationships in the Si3N4-SiO2-YbN-Yb2O3 system at 1500°C after Hampp et al. [39].

The reason for the instability of the apatite- ($Y_{10}(SiO_4)_6N_2$), wollastonite- ($YSiO_2N$), and melillite ($Y_2Si_3O_3N_4$) phases is the smaller cation radius of the Yb^{3+} ion (85.8 pm) in comparsion to Y^{3+} (89.3 pm) [40]. A detailed analysis of the different crystal structures of the four quasiquaterny phases in the Y-related system showed that the wöhlerite phase ($Yb_4Si_2O_7N_2$) is the only structure which can tolerate a wide variation of the radii of interstitial

cations. The mellilite structure is based on SiO_4-tetrahedron layers connected by cations (e.g. Y^{3+}) and the wollastonite structure consists of SiO_4-chains also connected by cations such as Y^{3+}. In the case of very small cations, the resulting narrow distance between the SiO_4-layers and -chains, respectively, causes a repulsive force between the SiO_4-tetrahedron and both structures became unstable.

Similar considerations are possible for the apatite phase, which would be the most interesting one in these system due to the relative good oxidation resistance (low nitrogen content) and the possibility of incorporation of cation impurities from the starting powders. Ito [41] reported a lower boundary of 89 pm for the interstitial cation radius in hydroxyapatites. These results fit quite well with the oberservations of Hampp, et al. [39] that the N-apatite is stable in the Y-system (Y^{3+}= 89.3 pm), but not in the Yb-system (Yb^{3+} = 85.8 pm).

MECHANICAL PROPERTIES

Silicon nitride-based ceramics have a bending strength at room temperature between 600 and 1000 MPa and a fracture toughness of 5-10 MPa$\sqrt{m}$. Most Si_3N_4 compositions exhibit a strong decrease in bending strength in the temperature range of 1000°C to 1200°C, as indicated for material A in Fig. 9. At this point, many research activitives are focussed on the development of high-strength Si_3N_4 ceramics which reveal only a small degradation up to 1500°C such as material B in Fig. 9. The following chapter is an attempt to show the influence of different parameters on the mechanical properties of Si_3N_4-based materials.

The bending strength and the fracture toughness at moderate temperatures is mainly influenced by the morphology of the Si_3N_4 grains and the flaw size. The typical fracture mode for Si_3N_4 ceramics is intergranular. The high fracture toughness values are due to deflection of the crack front by the elongated grains. High aspect ratio Si_3N_4 needles embedded in a fine-grained matrix with equiaxed grains are therefore desirable. Figure 10 shows plasma-etched micro-structures of Si_3N_4 ceramics with different average grain sizes and different aspect ratios of the elongated grains. The fine-grained material exhibits a

mean bending strength of more than 1000 MPa, whereas the sample with larger average grain size shows a strength of only 750 MPa. The composition of the sintering additives plays no significant role in the mechanical properties at low temperatures.

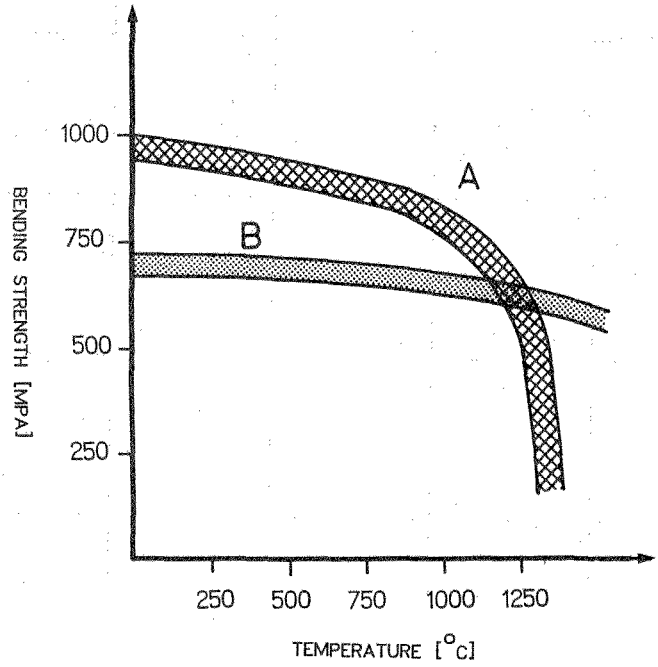

Figure 9: Schematic of typical bending strength vs temperature curves for Si_3N_4 ceramics.

In contrast to the room temperature properties, the bending strength at tempe ratures > 1000°C is mainly influenced by the chemistry of the grain boundary. The crystallisation of the amorphous grain boundary phase offers one possibilty for improving these properties. However, the devitrified material often exhibits only a slight improvement in the high temperature properties and a simultaneous decrease at room temperature. The effect can be explained by a volume misfit between the amorphous and the crystalline secondary phase or by a misfit in thermomechanical properties of the grain boundary phase and matrix. For example, a misfit in the thermal expansion coefficient causes stresses within the material and, in extreme cases, pre-damaging. The improvement in the high temperature properties by devitrification of the amorphous grain boundary also depends on the crystal structure of the secondary phase. A

crystal structure with large interstitial sites is desirable, so that impurities in the starting powders can be accommodated into the crystal lattice.

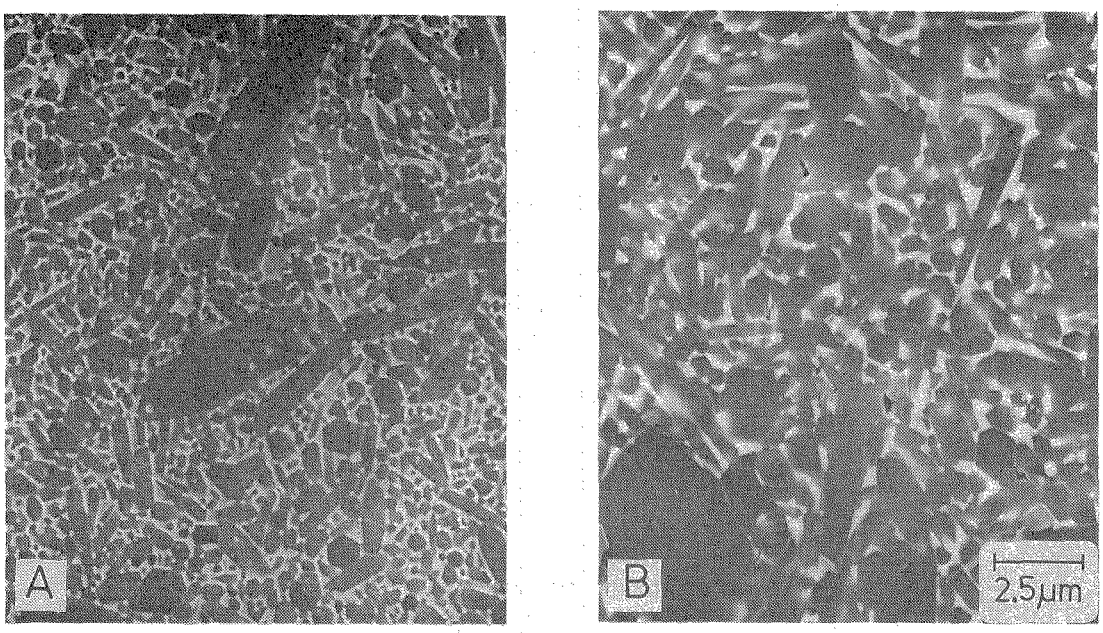

Figure 10: Typical microstructure of a Si_3N_4 ceramic with a bending strength of 1000 MPa (A) and 750 MPa (B).

In contrast, if the impurities remain in the residual amorphous phase, the softening point of the glass will be reduced and the high temperature properties may decrease in comparison to the material without a devitrified secondary phase.

As indicated in Fig. 11, a complete crystallisation of the grain boundaries is not possible. The high resolution TEM micrograph shows an amorphous layer of about 15 Å in the contact area between two Si_3N_4 grains with different orientations [42].

The chemical composition of these grain boundary films may have a strong influence on high temperature properties, such as bending strength and creep resistance. The equilibrium thickness of the film varies with the chemistry and depends therefore on the impurities and the sintering additives. The grain boundary film should be as thin as possible and the properties of the material could be improved by an amorphous grain boundary material with high viscosity.

ıere are also indications in recent work by Clarke [43], who studied the ·ain boundary films at high temperatures, that the equilibrium grain boundary ıickness changes above > 1000°C.

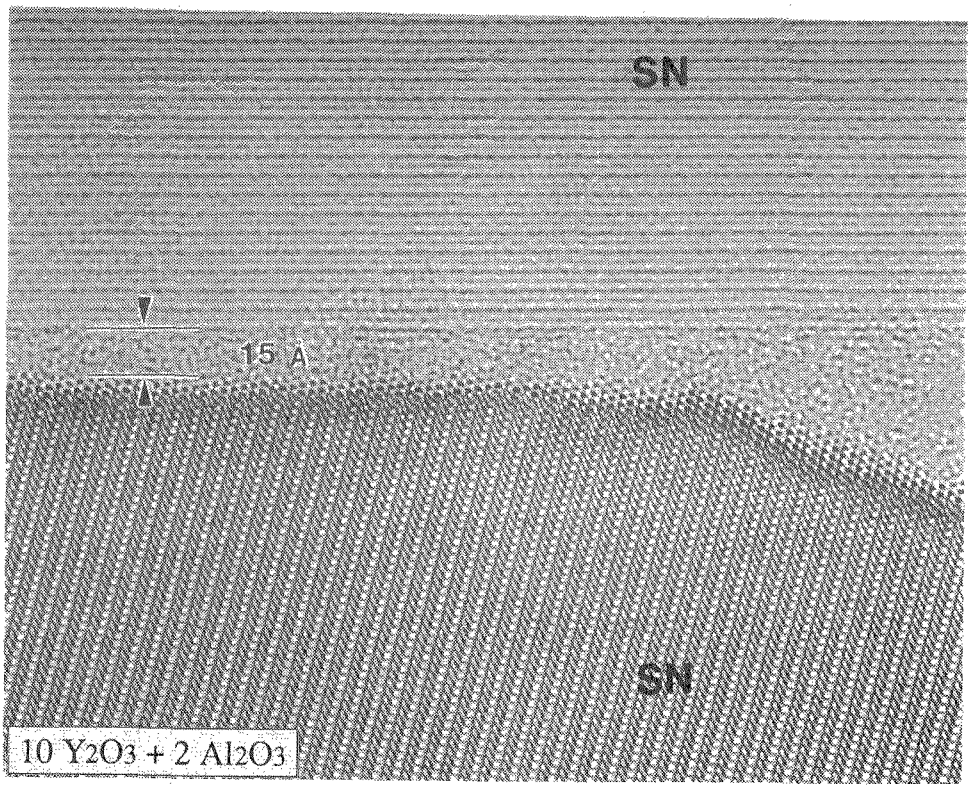

.gure 11: High resolution TEM micrograph indicating the amorphous grain boundary film [42].

JMMARY

ıe microstructural development of Si_3N_4-based ceramics have been studied. :periments revealed that the aspect ratio of the Si_3N_4 grains is controlled / the α/β ratio in the Si_3N_4 starting powder. Sintering studies on α-Si_3N_4)wder, doped with 5 vol.% coarse α-grains show that the homogeneous and :terogeneous nucleation on α-grains plays no important role.

ıe anisotropic grain growth behaviour was explained by a crystallisation)del on the basis of Kossel and Stransky. The different boundary energies of ıe prism- and basal plane could be derived from the β-Si_3N_4 crystal :ructure.

The mechanical properties of Si_3N_4 at room temperature are controlled by the microstructure, whereas at temperatures > 1000°C the chemistry of the grain boundary dominates. It was demonstrated that the knowledge of the phase relationships between sintering additives and Si_3N_4 is necessary for controllable crystallisation. The high temperature properties after devitrification depend strongly on the thermophysical properties of the crystalline second phase. High volume misfits and catastrophic oxidation behaviour can result in a decrease in the properties. TEM observations reveal that there is no possibility for complete grain boundary crystallisation.

REFERENCES

[1] K.Kijama and S.Shirasaki, "Nitrogen Self Diffusion in Silicon Nitride" J.Chem.Phys, **65**, 2668-71, (1976).

[2] G.C.Deeley, J.M.Herbert and N.C.Moore, "Dense Silicon Nitride", Pow.Met. **8**, 145-47, (1961).

[3] G.R. Terwillinger and F.F. Lange, "Pressureless Sintering of Si_3N_4", J.Mater.Sci., **10**, 1169-73, (1975).

[4] S.Boskovic, L.J.Gaukler G.Petzow and T.Y.Tien, "Reaction Sintering Forming β-Si_3N_4 Solid Solutions in the System Si,Al/N,O - I. Sintering of SiO_2-AlN-Mixtures" Pow.Met., **9**, 185-89, (1977).

[5] M. Mitomo, "Pressure Sintering of Si_3N_4", J.Mat.Sci., **11**, 1103-06, (1976).

[6] K.Negita, "Effective Sintering Aids for Si_3N_4 Ceramics", J.Mat.Sci. Letters, **4**, 755-758, (1985).

[7] K.Negita, "Ionic Radii and Electronegatives of Effective Sintering Aids for Si_3N_4 Ceramics", J.Mat.Sci.Letters, **4**, 417-418, (1985).

[8] M.Peukert and P.Greil, "Oxygen Distribution in Silicon Nitride Powders", J.Mat.Sci., **22**, 3717-20, (1987).

[9] J.Weiss and W.A.Kaysser, "Liquid Phase Sintering", in F.L.Riley (ed.), "Progress in Nitrogen Ceramics", 169-186, (1983).

[10] P.Greil, J. Bressani, and G. Petzow, "Crystallisation of Y-Al- Garnet in Pressureless Sintered β-SiAlON Materials", in: S.Somiya et al. (eds.), Proc.Int.Symp.on Ceramic Component for Eng., Tokyo, (1983), 228-35.

[11] E. Butler, R.J. Lumby, A. Szweda and M.Lewis, "Syalon Ceramics for High Temperature Engines; An Illustration of Grain Boundary Engineering", in: S.Somiya et al. (eds.), Proc.Int.Symp.on Ceramic Component for Eng., Tokyo, (1983), 159-69.

[12] Y. Oyama, O. Kamigaito, "Solid Solubility of some Oxides in Si_3N_4", Japan.J.Appl.Phys., 1673, (1971).

[13] Y. Oyama, "Solid Solution in the System Si_3N_4-Ga_2O_3-Al_2O_3", Japan.J.Appl. Phys., **12**, 500-8, (1973).

[14] K.H.Jack and W.J.Wilson, "Ceramics Based on the Si-Al-O-N Related Systems", Nature.Phys.Science, **238**, 28-29, (1982).

[15] J.Huseby, H.L.Lukas, G.Petzow, "Phase Equillibria in the System Si_3N_4-SiO_2-BeO-Be_2N_3", J.Am.Ceram.Soc., **58**, 377-80, (1975).

[16] D. Stutz, P. Greil, G. Petzow, "Two-dimensional Solid-Solution Formation of Y-containing α-Si_3N_4", J.Mat.Sci.Letters, **5**, 335-36, (1986).

[17] K.H. Jack, "The Crystal Chemistry of the SiAlONs and Related Ceramics", in F.L. Riley (ed.), "Progress in Nitrogen Ceramics", Martinus Nijhoff Publ., Boston, 109-26, (1983).

[18] M.Mitomo, H.Tanaka, U.Muramatsu and Y.Futjii, "The Strength of α-SiAlON Ceramics", J.Mater.Sci.Letters, **15**, 2661-62, (1980).

[19] C.Greskovich and G.E.Gazza, "Hardness of dense α- and β-Si_3N_4 Ceramics", J.Maters.Sci.Letters, **4**, 195-96, (1985).

[20] E. Tani, S. Umebayashi, K. Kishi, K. Kobayashi and M. Nishijima, "Gas Pressure Sintering of Si_3N_4 with Concurrent Addition of Al_2O_3 and 5wt.% Rare Earth Oxide: High fracture Toughness Si_3N_4 with Fiber-like Structure", Am.Ceram.Bull., **65**, (1986), 1311-15.

[21] M.J.Hoffmann, A.Nagel, P.Greil and G.Petzow, "Slip Casting of SiC-Whisker-Reinforced Si_3N_4", J.Am. Ceram.Soc., **72**, 765-69, (1989).

[22] M.J.Hoffmann, P. Greil and G.Petzow, "Pressureless Sintering of SiC-Whisker-Reinforced Si_3N_4" in: D.Taylor (ed.), "Science of Ceramics", **14**, Stoke-on-Trent, UK, 825-30, (1987).

[23] F.F.Lange, "Fracture Toughness of Si_3N_4 as a Function of the Initial α-Phase Content", J.Am.Ceram.Soc., **62**, 428-30, (1979).

[24] K.T.Faber and A.G.Evans, "Crack Deflection Processes - I. Theory", Acta. metall. **31**, 565-67, (1983).

[25] H.Liu, K.L.Weißkopf and G.Petzow, "Crack Deflection Process for Hot-Pressed Whisker-Reinforced Ceramic Composites", J.Am.Ceram.Soc., **72**, 559-563, (1989).

[26] W. Dreßler, M.J. Hoffmann, and G. Petzow, "Analysis of Microstructural Development in Si_3N_4 Ceramics", to be published.

[27] M. Krämer, "Investigations of the Growth Kinetics of β-Si_3N_4 in Ceramics and Oxynitride Glasses", Ph.D. Thesis (in German), University Stuttgart, (1991).

[28] W. Kossel, "To the Theory of Crystal Growths" (in German), Naturw. Ges. Göttingen, **2**, 135-39, (1927).

[29] D. Hardie and K.H. Jack, "Crystal Structures of Silicon Nitride", Nature, **180**, 332-33, (1957).

[30] G.Wötting, B.Kanka, G.Ziegler, "Microstructural Development, Microstructural Characterization and relation to Mechanical Properties of Dense Silicon Nitride", in: Stuart Hampshire (ed.), "Non-Oxide Technical and Engineering Ceramics", Elsevier Appl.Sci.Pub. Ltd, London - New York, 83-96, (1986).

[31] M. Krämer, M.J. Hoffmann, and G. Petzow, "Growth of Si_3N_4 Dispersed in Oxinitride Glass", to be published.

[32] L.J.Gaukler and G.Petzow, "Representation of Multicomponent Silicon Nitride Based System" in: "Nitrogen Ceramics", NATO Advanced Study Institute, Canterbury, UK, (1976).

[33] K.H. Jack, "Crystal Chemistry, Stochiometry, Spinodal Decomposition, Properties of Inorganic Phases", in: A.M. Alper (ed.) "Phase Diagrams: Materials Science and Technology, Vol. 5, Academic Press, New York, 242-47, (1978).

[34] D.P. Thompson, "Phase Relationships in Y-Si-Al-O-N Ceramics", in: R.T. Tressler et al. (eds.), "Tailoring Multiphase and Composite Ceramics", Plenum Publ. Corporation, 79-91, (1986).

[35] L.J.Gaukler, H.Hohnke and T.Y.Tien, "The System Si_3N_4-SiO_2-Y_2O_3", J.Amer. Ceram.Soc., **63**, 35-37, (1980).

[36] J.K.Patel and D.P.Thompson, "The Low-temperature Oxidation Problem in Yttria-Densified Silicon Nitride Ceramics", Br.Ceram.Trans.J.,**87**, 70-73, (1988).

[37] F.F. Lange, S.C. Singhal and R.C. Kuznicki, "Phase Relationships and Stability Studies in the S_3N_4-SiO_2-Y_2O_3 Pseudoternary System", J.Amer. Ceram.Soc., **60**, 249-52, (1977).

[38] C.L. Quackenbush and J.T. Smith, "Phase Effects in Si_3N_4 Containing Y_2O_3 or CeO_2: II, Oxidation", Am. Ceram.Soc.Bull., **59**, 532-37, (1980).

[39] E. Hampp, M.J. Hoffmann, and G. Petzow, "Phase Relationships in the System S_3N_4-SiO_2-Yb_2O_3", to be published.

[40] R.C. Weast, M.J. Astle, W.H. Beyer, "CRC Handbook of Chemistry and Physics", CRC Press, Boca Raton, Florida, (1987), F-157.

[41] J.Ito, "Silicate Apatites and Oxyapatites", Am.Mineral., **53**, 890-95, (1968).

[42] A. Kleebe et al., "Grain Boundary Film Thickness in Si_3N_4", to be published in J.Euro.Ceram.Soc., May 1992.

[43] David R. Clarke, "High-Temperature Microstructure of a Hot-Pressed Silicon Nitride", J.Am.Ceram.Soc., **72**, 1604-09, (1989).